Box-constrained Total-variation Image Restoration with Automatic Parameter Estimation

HE Chuan[1] HU Chang-Hua[1] ZHANG Wei[1] SHI Biao[1]

Abstract The box constraints in image restoration have been arousing great attention, since the pixels of a digital image can attain only a finite number of values in a given dynamic range. This paper studies the box-constrained total-variation (TV) image restoration problem with automatic regularization parameter estimation. By adopting the variable splitting technique and introducing some auxiliary variables, the box-constrained TV minimization problem is decomposed into a sequence of subproblems which are easier to solve. Then the alternating direction method (ADM) is adopted to solve the related subproblems. By means of Morozov′s discrepancy principle, the regularization parameter can be updated adaptively in a closed form in each iteration. Image restoration experiments indicate that with our strategies, more accurate solutions are achieved, especially for image with high percentage of pixel values lying on the boundary of the given dynamic range.

Key words Total variation (TV), box constraints, variable splitting, alternating direction method (ADM)

Citation He Chuan, Hu Chang-Hua, Zhang Wei, Shi Biao. Box-constrained total-variation image restoration with automatic parameter Estimation. *Acta Automatica Sinica*, 2014, **40**(8): 1804−1811

DOI 10.3724/SP.J.1004.2014.01804

The past few decades have witnessed the mushroom of the digital image restoration in a variety of fields[1], including remote sensing, astronomy, medical imaging, etc. Generally speaking, during acquisition and transmission, digital images are often degraded to be defective or even unusable, due to the defocusing of the lens system, the relative motion between the camera and the scene, or the all-pervasive noise. Recovering an estimate of the original scene from the degraded observation is the aim of image restoration.

In general, the degradation of an image can be described as the following linear system. First, the original image is convolved by a spatially invariant point spread function (PSF), and then, the result is contaminated with some type of noise, e.g., Gaussian, Poisson, gamma or impulse noise. The Gaussian noise is the most frequently used assumption and it is reasonable in many situations. With the Gaussian noise and the spatially invariant PSF assumptions, the image restoration task seems easy to accomplish. But unfortunately, even if the PSF is known or can be estimated exactly, the estimation of the original scene is an ill-posed linear inverse problem (IPLIP), and the solution is highly sensitive to the noise existing in the observed image. Thus, the inverse filtering, which tries to directly restore the original image, usually results in an estimate of no usability. To achieve a satisfactory restoration result, some prior knowledge of the original image is required and this results in the regularization of the IPLIP.

Among various regularization methods, the total-variation (TV)[2] regularization is remarkable for its attractive edge preservation ability[2−3]. However, the classical TV model has not considered the given dynamic range of a digital image. Actually, the pixels of a digital image can attain only a finite number of values (e.g., an 8-bit image can only have 256 gray levels). Thus if one would like to restore an image within some dynamic range (e.g., in [0, 255]), the imposition of box constraints becomes necessary. So far, a few works in the literature have considered the box constraints[4−8] and some others have considered easier positive constraints[9−11] in image restoration. As mentioned in [8], the restoration result of the box-constrained TV-regularized method is better than that of the classical TV-regularized method, especially when there are many pixels with valves lying on the boundary of the dynamic range in the original image.

Besides the box constraints, the estimation of the regularization parameter, which balances the regularization term and the data-fidelity term, is essential for successfully solving the TV restoration problem. It is well known that the solution of the TV model suffers a lot from its nondifferentiability, and the automatic estimation of the regularization parameter will bring in much more extra computation cost. Therefore, most papers in the literature just considered a fixed regularization parameter which was selected in a manual way. However, the automatic estimation of the regularization parameter is essential, because in many practical application cases, a wholly automatic way but not a human-computer interaction way is required.

Up to now, some efforts have been made on the automatic estimation of the regularization parameter[12−20]. Among these methods, Morozov′s discrepancy principle is a good choice when the noise level is accessible[12−15]. In order to make use of the existing methods with a fixed regularization parameter, Blomgren and Chan[16] proposed a modular solver. Afonso et al.[14] achieved the adaptive restoration of the original image, by embedding Chambolle′s dual method[21] into the alternating direction method of multipliers (ADMM). In [15], the primal-dual model of TV was adopted to restore the blurred image and the Newton′s inner iteration scheme was applied to update the regularization parameter. The similar use of the Newton′s iteration scheme can also be found in [12] and [13]. Although an automatic estimation of the regularization parameter is achieved in these methods, they all involve an inner iteration scheme. Thus, much extra computing cost is introduced.

In this paper, we propose an algorithm to solve the box-constrained TV restoration problem with automatic regularization parameter estimation. By resorting to the variable splitting technique, the box-constrained TV-regulari-

Manuscript received August 29, 2013; accepted March 24, 2014
Supported by National Natural Science Foundation of China (61174030, 61104223, 61203189, 61374120, 61203007), the Postdoctoral Science Foundation of China (2012M512147), and National Science Fund for Distinguished Young Scholars of China (61025014)
Recommended by Associate Editor ZHOU Jie
1. Hi-Tech Institute of Xi′an, Xi′an 710025, China

zed problem is decomposed into a sequence of subproblems that are much easier to solve. Then the alternating direction method (ADM) is used to solve these subproblems. In each iteration, the regularization parameter is adaptively updated in a closed form. In fact, our method can also be seen as an instance of the ADMM.

Two aspects distinguish our method from the other results in the literature. On the one hand, in contrast with [4−8], which addressed the box-constrained TV restoration with a fixed predetermined regularization parameter, our algorithm achieves the automatic estimation of this parameter. On the other hand, compared with the methods which adaptively handle the classical TV restoration problem with inner iterations[12−15], our algorithm allows the box constraints and updates the parameter in a closed form. With no inner iteration, the computation cost of our algorithm is lower compared with algorithms with inner iterations.

This paper is organized as follows. In Section 1, the problem formulation is established. Section 2 offers the derivation leading to the proposed algorithm and some practical parameter setting tricks. Numerical experiments for demonstration are presented in Section 3. Finally, Section 4 summarizes this paper.

1 Problem formulation

We assume that the images used throughout this paper have an $m \times n$ domain, and are denoted as mn vectors formed by stacking up the image matrix rows. Therefore, the $(i,\ j)$th image pixel becomes the $((i-1)\times n+j)$th entry of the vector. Then, the image degradation process can be modeled as the following discrete linear problem

$$\boldsymbol{f} = K\boldsymbol{u}_{\rm clean} + \boldsymbol{n} \tag{1}$$

where $\boldsymbol{f}$ and $\boldsymbol{u}_{\rm clean}$ are vector presentations of the observed image and original image, respectively; K is the convolution operator resulted from the spatially invariant PSF, which is assumed to be known; $\boldsymbol{n}$ is the vector of Gaussian white noise with variance σ^2.

Denote the Euclidean space $\mathbf{R}^{mn}$ as V, and define $Q = V \times V$. The ith components of $\boldsymbol{x} \in V$ and $\boldsymbol{y} \in Q$ are denoted as $x_i \in \mathbf{R}$ and $\boldsymbol{y}_i = (y_i^{(1)},\ y_i^{(2)})^{\rm T} \in \mathbf{R}^2$, respectively. Define inner products and Euclidean norms in V and Q as

$$\begin{aligned}&\langle \boldsymbol{x},\ \boldsymbol{x}\rangle_V = \sum_i^{mn} x_i x_i,\quad \|\boldsymbol{x}\|_2 = \sqrt{\langle \boldsymbol{x},\ \boldsymbol{x}\rangle_V}\\ &\langle \boldsymbol{y},\ \boldsymbol{y}\rangle_Q = \sum_i^{mn}\sum_{k=1}^{2} y_i^{(k)} y_i^{(k)},\quad \|\boldsymbol{y}\|_2 = \sqrt{\langle \boldsymbol{y},\ \boldsymbol{y}\rangle_Q}\end{aligned} \tag{2}$$

For each $\boldsymbol{u} \in V$, define $D_i\boldsymbol{u} = [(D^{(1)}\boldsymbol{u})_i,\ (D^{(2)}\boldsymbol{u})_i]^{\rm T}$, where $D^{(1)},\ D^{(2)} \in \mathbf{R}^{mn\times mn}$ are $mn \times mn$ gradient matrices in the vertical and horizontal directions. $D_i \in \mathbf{R}^{2\times mn}$ is a tow-row matrix formed by stacking the ith rows of $D^{(1)}$ and $D^{(2)}$ together. Define the global first-order finite difference operator as $D = [(D^{(1)})^{\rm T},\ (D^{(2)})^{\rm T}]^{\rm T} \in \mathbf{R}^{2mn\times mn}$ and we consider $D\boldsymbol{u} \in Q$. Besides, we assume the periodic boundary condition of images in this paper.

With the above notations, the box-constrained TV restoration problem with a fixed regularization parameter can be described as follows

$$\min_{\boldsymbol{u}} \sum_i^{mn} \|D_i\boldsymbol{u}\|_2 + \frac{\lambda}{2}\|K\boldsymbol{u} - \boldsymbol{f}\|_2^2, \quad \text{s.t.} \quad \boldsymbol{u} \in \Omega \tag{3}$$

where $\boldsymbol{u}$ denotes the estimate of $\boldsymbol{u}_{\rm clean}$. $\Omega = \{\boldsymbol{u} \in \mathbf{R}^{mn} | \boldsymbol{p} \le \boldsymbol{u} \le \boldsymbol{q}\}$ with $\boldsymbol{p}, \boldsymbol{q} \in \mathbf{R}_+^{mn}$ is the box constraint imposed on $\boldsymbol{u}$ and it should be interpreted entry-wise. The first term in (3) is the TV semi-norm of $\boldsymbol{u}$, whereas the second term is the data-fidelity term. λ is the so-called regularization parameter which plays the role of making a compromise between the TV regularizer and the data-fidelity term.

The adaptive box-constrained TV restoration problem considered in this paper can be described as follows

$$\min_{\boldsymbol{u}} \sum_i^{mn} \|D_i\boldsymbol{u}\|_2 \quad \text{s.t.} \quad \boldsymbol{u} \in \{\Omega \cap \Psi\} \tag{4}$$

where $\Psi = \{\boldsymbol{u} \in \mathbf{R}^{mn} | \|K\boldsymbol{u} - \boldsymbol{f}\|_2^2 \le c\}$ is the feasible set constraint in accordance with Morozov′s discrepancy principle, where the upper bound $c = \tau mn\sigma^2$ is a predetermined noise-dependent parameter. In fact, by the classical Lagrangian method of multipliers, given a c, there exists a $\lambda \ge 0$ such that (4) and (3) are equivalent. Further, let $\delta_\Omega(\boldsymbol{u})$ signify the indicator function of set Ω, i.e., if $\boldsymbol{u} \in \Omega$, $\delta_\Omega(\boldsymbol{u}) = 0$; or else $\delta_\Omega(\boldsymbol{u}) = \infty$. Then, we can rewrite the adaptive box-constrained TV restoration problem (4) in an unconstrained form as follows

$$\min_{\boldsymbol{u}} \sum_i^{mn} \|D_i\boldsymbol{u}\|_2 + \delta_\Omega(\boldsymbol{u}) + \delta_\Psi(\boldsymbol{u}) \tag{5}$$

2 Methodology

2.1 Variable splitting and augmented Lagrangian function for TV restoration problem

Although problems (4) and (5) seem simple from appearance, the solution of them is troublesome due to the nondifferentiability of the TV norm and the existence of box constraints. So far, several approaches have been proposed to overcome the nondifferentiability of the TV regularizer, including time-marching method[2], primal-dual based algorithms[15, 22], variable splitting schemes[23−27], etc. Here, we adopt the variable splitting technique and the following discussion will show its advantage.

Referring to variable splitting, we introduce three auxiliary variables, i.e., an auxiliary variable $\boldsymbol{x}$ for liberating $K\boldsymbol{u}$ out of the restriction of the discrepancy principle, an auxiliary variable $\boldsymbol{y}$ (or $\boldsymbol{y}_i$ for $D_i\boldsymbol{u}$, respectively) for liberating $D\boldsymbol{u}$ out of nondifferentiability, and an auxiliary variable $\boldsymbol{z}$ for liberating $\boldsymbol{u}$ out of the restriction of the box constraints. With these three auxiliary variables, the minimization functional (5) is equivalent to the following linear constrained problem

$$\begin{aligned}&\min_{\boldsymbol{x},\boldsymbol{y},\boldsymbol{z}} \sum_i^{mn} \|\boldsymbol{y}_i\|_2 + \delta_\Phi(\boldsymbol{x}) + \delta_\Omega(\boldsymbol{z})\\ &\text{s.t.}\ \ K\boldsymbol{u} = \boldsymbol{x},\ \ D\boldsymbol{u} = \boldsymbol{y},\ \ \boldsymbol{u} = \boldsymbol{z}\end{aligned} \tag{6}$$

where $\delta_\Phi(\boldsymbol{x})$ is the indicator function of set $\Phi = \{\boldsymbol{x} \in \mathbf{R}^{mn} | \|\boldsymbol{x} - \boldsymbol{f}\|_2^2 \le c\}$. The augmented Lagrangian functional for minimization problem (6) is defined as

$$\begin{aligned}\mathcal{L}_A(\boldsymbol{u},\boldsymbol{x},\boldsymbol{y},\boldsymbol{z};\boldsymbol{\mu},\boldsymbol{\xi},\boldsymbol{\eta}) = \delta_\Phi(\boldsymbol{x}) - \boldsymbol{\mu}^{\rm T}(\boldsymbol{x} - K\boldsymbol{u}) +\\ \frac{\beta_1}{2}\|\boldsymbol{x} - K\boldsymbol{u}\|_2^2 + \sum_i^{mn}\|\boldsymbol{y}_i\|_2 - \boldsymbol{\xi}^{\rm T}(\boldsymbol{y} - D\boldsymbol{u}) +\end{aligned}$$

$$\frac{\beta_2}{2}\|\boldsymbol{y}-D\boldsymbol{u}\|_2^2+\delta_\Omega(\boldsymbol{z})-\boldsymbol{\eta}^{\mathrm{T}}(\boldsymbol{z}-\boldsymbol{u})+\frac{\beta_3}{2}\|\boldsymbol{z}-\boldsymbol{u}\|_2^2 \tag{7}$$

where $\boldsymbol{\mu}$, $\boldsymbol{\eta}\in V$ and $\boldsymbol{\xi}\in Q$ are Lagrange multipliers. β_1, β_2, and β_3 are positive penalty parameters. Denote the saddle point of $\mathcal{L}_A$ as $(\boldsymbol{u}^*,\boldsymbol{x}^*,\boldsymbol{y}^*,\boldsymbol{z}^*,\boldsymbol{\mu}^*,\boldsymbol{\xi}^*,\boldsymbol{\eta}^*)$. Then, according to the augmented Lagrangian theory, the solution of problem (6) is equivalent to $(\boldsymbol{u}^*, \boldsymbol{x}^*, \boldsymbol{y}^*, \boldsymbol{z}^*)$.

2.2 Deduction of the proposed algorithm

The augmented Lagrangian method (ALM) iterates between minimizing $\mathcal{L}_A$ with respect to $(\boldsymbol{u}, \boldsymbol{x}, \boldsymbol{y}, \boldsymbol{z})$ (keeping the multipliers $\boldsymbol{\mu}$, $\boldsymbol{\xi}$, and $\boldsymbol{\eta}$ fixed) and updating the multipliers, until some convergence criterion is satisfied. The problem yielding $(\boldsymbol{u}, \boldsymbol{x}, \boldsymbol{y}, \boldsymbol{z})$ exactly in ALM needs an inner iteration scheme. In fact, setting the inner iteration number to 1 (in this case, the ALM becomes the so-called ADM) is adequate for the convergence of ALM. Since when the inner iteration number is larger than 1, the accuracy of the inner iteration will be wasted by the outer iteration[27]. To find the minimizer of (6), we resort to ADM, and this yields the iteration scheme as follows

$$\boldsymbol{u}^{k+1}=\arg\min_{\boldsymbol{u}}\mathcal{L}_A\left(\boldsymbol{u},\boldsymbol{x}^k,\boldsymbol{y}^k,\boldsymbol{z}^k;\boldsymbol{\mu}^k,\boldsymbol{\xi}^k,\boldsymbol{\eta}^k\right) \tag{8}$$

$$\boldsymbol{y}^{k+1}=\arg\min_{\boldsymbol{y}}\mathcal{L}_A\left(\boldsymbol{u}^{k+1},\boldsymbol{x}^k,\boldsymbol{y},\boldsymbol{z}^k;\boldsymbol{\mu}^k,\boldsymbol{\xi}^k,\boldsymbol{\eta}^k\right) \tag{9}$$

$$\boldsymbol{x}^{k+1}=\arg\min_{\boldsymbol{x}}\mathcal{L}_A\left(\boldsymbol{u}^{k+1},\boldsymbol{x},\boldsymbol{y}^{k+1},\boldsymbol{z}^k;\boldsymbol{\mu}^k,\boldsymbol{\xi}^k,\boldsymbol{\eta}^k\right) \tag{10}$$

$$\boldsymbol{z}^{k+1}=\arg\min_{\boldsymbol{z}}\mathcal{L}_A\left(\boldsymbol{u}^{k+1},\boldsymbol{x}^{k+1},\boldsymbol{y}^{k+1},\boldsymbol{z};\boldsymbol{\mu}^k,\boldsymbol{\xi}^k,\boldsymbol{\eta}^k\right) \tag{11}$$

$$\boldsymbol{\mu}^{k+1}=\boldsymbol{\mu}^k-\beta_1\left(\boldsymbol{x}^{k+1}-K\boldsymbol{u}^{k+1}\right) \tag{12}$$

$$\boldsymbol{\xi}^{k+1}=\boldsymbol{\xi}^k-\beta_2\left(\boldsymbol{y}^{k+1}-D\boldsymbol{u}^{k+1}\right) \tag{13}$$

$$\boldsymbol{\eta}^{k+1}=\boldsymbol{\eta}^k-\beta_3\left(\boldsymbol{z}^{k+1}-\boldsymbol{u}^{k+1}\right) \tag{14}$$

From the above seven iterative equations, we can find that only the updating of variable $\boldsymbol{x}$ is restricted to the discrepancy principle, i.e., only variable $\boldsymbol{x}$ is in relationship with the regularization parameter λ.

The minimization subproblem (8) with respect to $\boldsymbol{u}$ has a least-square form style as follows

$$\left(\frac{\beta_1}{\beta_2}K^{\mathrm{T}}K+D^{\mathrm{T}}D+\frac{\beta_3}{\beta_2}I\right)\boldsymbol{u}=\frac{\beta_1}{\beta_2}K^{\mathrm{T}}\left(\boldsymbol{x}^k-\frac{\boldsymbol{\mu}^k}{\beta_1}\right)+ D^{\mathrm{T}}\left(\boldsymbol{y}^k-\frac{\boldsymbol{\xi}^k}{\beta_2}\right)+\frac{\beta_3}{\beta_2}\left(\boldsymbol{z}^k-\frac{\boldsymbol{\eta}^k}{\beta_3}\right) \tag{15}$$

so that it has a closed form solution. Under the periodic boundary condition, matrices K, $D^{(1)}$, and $D^{(2)}$ are block-circulant, and therefore, they can be diagonalized by the discrete Fourier transform (DFT) matrix. As mentioned in [28], equation in the form of (15) can be solved by two FFTs and one inverse FFT in $\mathrm{O}(mn\log(mn))$ multiplicative operations.

The solution to subproblem (9) with respect to $\boldsymbol{y}$ is given explicitly by the two-dimensional shrinkage[28]

$$\boldsymbol{y}_i^{k+1}=\max\left\{\left\|D_i\boldsymbol{u}^{k+1}+\frac{\boldsymbol{\xi}_i^k}{\beta_2}\right\|_2-\frac{1}{\beta_2},0\right\}\times \frac{D_i\boldsymbol{u}^{k+1}+\frac{\boldsymbol{\xi}_i^k}{\beta_2}}{\left\|D_i\boldsymbol{u}^{k+1}+\frac{\boldsymbol{\xi}_i^k}{\beta_2}\right\|_2} \tag{16}$$

where "$\times$" should be interpreted component-wise and the convention $0\times(0/0)=0$ is assumed. The computational cost of (16) is linear with mn.

The subproblem with respect to $\boldsymbol{x}$ can be written as

$$\boldsymbol{x}^{k+1}=\arg\min_{\boldsymbol{x}}\delta_\Phi(\boldsymbol{x})-\left(\boldsymbol{\mu}^k\right)^{\mathrm{T}}\boldsymbol{x}+\frac{\beta_1}{2}\left\|\boldsymbol{x}-K\boldsymbol{u}^{k+1}\right\|_2^2= \arg\min_{\boldsymbol{x}}\frac{\lambda^{k+1}}{2}\|\boldsymbol{x}-\boldsymbol{f}\|_2^2+\frac{\beta_1}{2}\left\|\boldsymbol{x}-\boldsymbol{a}^{k+1}\right\|_2^2 \tag{17}$$

where $\boldsymbol{a}^{k+1}=K\boldsymbol{u}^{k+1}+\boldsymbol{\mu}^k/\beta_1$, and λ^{k+1} is the estimated regularization parameter in the $(k+1)$th iteration which is consistent with the discrepancy principle. It is obvious that $\boldsymbol{x}$ is λ related, and in each iteration, we should check whether $\|\boldsymbol{x}-\boldsymbol{f}\|_2^2\le c$ holds.

The solutions of λ^{k+1} and $\boldsymbol{x}^{k+1}$ fall into two cases based on the range of $\boldsymbol{a}^{k+1}$. On the one hand, if $\|\boldsymbol{a}^{k+1}-\boldsymbol{f}\|_2^2\le c$ holds, we can set $\lambda^{k+1}=0$ and $\boldsymbol{x}^{k+1}=\boldsymbol{a}^{k+1}$ according to the theory of Lagrangian method. On the other hand, if $\|\boldsymbol{a}^{k+1}-\boldsymbol{f}\|_2^2>c$ holds, according to the same theory, we should solve the following equation

$$\left\|\boldsymbol{x}^{k+1}-\boldsymbol{f}\right\|_2^2=c \tag{18}$$

to make $\boldsymbol{x}^{k+1}$ satisfy Morozov's discrepancy principle. Since the minimization problem (17) is quadratic, it has a closed form solution as follows

$$\boldsymbol{x}^{k+1}=\frac{\lambda^{k+1}\boldsymbol{f}+\beta_1\boldsymbol{a}^{k+1}}{\lambda^{k+1}+\beta_1} \tag{19}$$

Substituting $\boldsymbol{x}^{k+1}$ with (19) into (18), we obtain

$$\lambda^{k+1}=\beta_1\frac{\|\boldsymbol{f}-\boldsymbol{a}^{k+1}\|_2}{\sqrt{c}}-\beta_1 \tag{20}$$

The subproblem of $\boldsymbol{z}$ is given by

$$\boldsymbol{z}^{k+1}=\arg\min_{\boldsymbol{z}}\delta_\Omega(\boldsymbol{z})-\left(\boldsymbol{\eta}^k\right)^{\mathrm{T}}\boldsymbol{z}+\frac{\beta_3}{2}\left\|\boldsymbol{z}-\boldsymbol{u}^{k+1}\right\|_2^2= \mathcal{P}_\Omega\left(\boldsymbol{u}^{k+1}+\frac{\boldsymbol{\eta}^k}{\beta_3}\right) \tag{21}$$

where $\mathcal{P}_\Omega$ denotes the projection operator onto set Ω and the solution of projection problem can be found in [29].

We summarize the above discussion in the following algorithm named automatic parameter estimation algorithm for box-constrained total-variation image restoration (APEA-BCTV).

Algorithm 1. APEA-BCTV (Automatic parameter estimation algorithm for box-constrained total-variation image restoration)

Input. $\boldsymbol{f}$, K, c.

1. Initialize $\boldsymbol{u}^0$, $\boldsymbol{x}^0$, $\boldsymbol{y}^0$, $\boldsymbol{z}^0$, $\boldsymbol{\mu}^0$, $\boldsymbol{\xi}^0$, $\boldsymbol{\eta}^0$. Set $k=0$, β_1, β_2, $\beta_3>0$.
2. **While** stopping criterion is not satisfied, **do**
3. Compute $\boldsymbol{u}^{k+1}$ according to (15);
4. Compute $\boldsymbol{y}^{k+1}$ according to (16);
5. **If** $\left\|\boldsymbol{a}^{k+1}-\boldsymbol{f}\right\|_2^2\le c$ holds **then**
6. $\lambda^{k+1}=0$ and $\boldsymbol{x}^{k+1}=\boldsymbol{a}^{k+1}$;
7. **Else**
8. Update λ^{k+1} and $\boldsymbol{x}^{k+1}$ according to (20) and (19);

Compute $\boldsymbol{z}^{k+1}$ according to (21);
End if
Update $\boldsymbol{\mu}^{k+1}$, $\boldsymbol{\xi}^{k+1}$, and $\boldsymbol{\eta}^{k+1}$ according to (12), (13), and (14);
$k = k + 1$;
End while
Return λ^{k+1} and $\boldsymbol{u}^{k+1}$.

In Algorithm 1, by introducing the auxiliary variable $\boldsymbol{x}$, we achieve the automatic update of λ without any inner iteration. This point makes our algorithm different from those in [12−16], which introduce inner iterations to achieve the update of the regularization parameter. Besides, by introducing $\boldsymbol{y}$ and $\boldsymbol{z}$, the TV norm is liberated out from nondifferentiability and variable $\boldsymbol{u}$ is liberated out from the box constraints. All these efforts simplify the solving of the box-constrained TV restoration problem.

The procedure for solving (15) corresponding to the $\boldsymbol{u}$ subproblem in the proposed algorithm consumes the most calculation, and therefore, the calculation cost of our algorithm is $\mathrm{O}(mn\log(mn))$ multiplicative operations. In fact, our algorithm is an instance of the classical ADMM, so its convergence can be guaranteed by the theorem of Wu and Tai in [27]. We summarize the convergence of the proposed algorithm by the following theorem.

Theorem 1. Given β_1, β_2, $\beta_3 > 0$, the sequence $\{\boldsymbol{u}^k, \boldsymbol{x}^k, \boldsymbol{y}^k, \boldsymbol{z}^k, \boldsymbol{\mu}^k, \boldsymbol{\xi}^k, \boldsymbol{\eta}^k, \lambda^k\}$ generated by Algorithm 1 from any initial point converges to $(\boldsymbol{u}^*, \boldsymbol{x}^*, \boldsymbol{y}^*, \boldsymbol{z}^*, \boldsymbol{\mu}^*, \boldsymbol{\xi}^*, \boldsymbol{\eta}^*, \lambda^*)$, where $(\boldsymbol{u}^*, \boldsymbol{x}^*, \boldsymbol{y}^*, \boldsymbol{z}^*, \boldsymbol{\mu}^*, \boldsymbol{\xi}^*, \boldsymbol{\eta}^*)$ is a saddle point of $\mathcal{L}_A$ with $\lambda = \lambda^*$. In particular, $(\boldsymbol{u}^*, \boldsymbol{x}^*, \boldsymbol{y}^*, \boldsymbol{z}^*)$ is a solution of functional (6), $\boldsymbol{u}^*$ is the minimizer of functional (4), and λ^* is the Lagrange multiplier corresponding to constraint $\boldsymbol{u} \in \Psi$.

The proof of Theorem 1 is similar to Wu and Tai′s convergence analysis for the classical ADMM. For simplicity, we do not repeat the lengthy deduction process here. However, we still emphasize the importance of Theorem 1, since it theoretically guarantees the convergence of APEA-BCTV.

2.3 Parameter setting

The noise-dependent upper bound c in the minimization functional (4) plays a very important role, since a good choice of this parameter suppresses the error between the original image and the restored image. As described above, $c = \tau mn\sigma^2$. Although many methods are available to estimate the noise variance, to our knowledge, the selection of c is still a pendent problem up to now, since the identification of parameter τ is much more difficult. Setting $\tau = 1$ has been a custom choice, but this choice may result in oversmoothed solution while the noise level is not high[15]. In this paper, by fitting experimental data with a straight line, we suggest setting

$$\tau = -0.006 \times \mathrm{BSNR} + 1.09 \tag{22}$$

A similar setting strategy can be found in [14]. In (22), the blurred signal-to-noise ratio (BSNR) is defined as follows

$$\mathrm{BSNR} = 10\lg \frac{\|\boldsymbol{f} - \bar{\boldsymbol{f}}\|_2^2}{mn\sigma^2} \tag{23}$$

where $\bar{\boldsymbol{f}}$ denotes the mean of the observed image $\boldsymbol{f}$. With the setting of parameter τ, the upper bound c can be easily calculated through $c = \tau mn\sigma^2$.

Besides the choice of the upper bound c, the setting of parameters β_1, β_2, and β_3 is important to our algorithm. By a large number of experiments, we suggest setting $\beta_1 = \beta_3 = 3\beta_2$, where $\beta_2 = 1$. In fact, $\beta_1 = \beta_2 = \beta_3 > 0$ is sufficient for the convergence of the proposed algorithm. However, by setting $\beta_1 = \beta_3 = 3\beta_2$, our algorithm can result in a more attractive result. Similar parameter settings can be found in some other ADMM based algorithms[8].

3 Numerical experiments

In this section, numerical experiments are presented to examine the applicability of the proposed algorithm to different varieties of images, different types of blur kernels, as well as different levels of noise. The experiments are performed under Matlab v7.8.0 and Windows 7 on a PC with Intel Core (TM) i5 CPU (3.20 GHz) and 8 GB of RAM. The quality of the restoration results is measured by the improved signal-to-noise ratio (ISNR) defined as follows

$$\mathrm{ISNR} = 10\lg \frac{\|\boldsymbol{f} - \boldsymbol{u}_{\mathrm{clean}}\|_2^2}{\|\boldsymbol{u} - \boldsymbol{u}_{\mathrm{clean}}\|_2^2} \tag{24}$$

The four test images are 256 × 256 images shown in Fig. 1. Their pixel values are all scaled to the interval [0, 255], and therefore, for the box constraints, we have $\boldsymbol{p} = \boldsymbol{0}$ and $\boldsymbol{q} = \boldsymbol{255}$. The percentages of extreme-value pixels in the four test images, i.e., pixels with value 0 or 255, are 100 %, 89.81 %, 28.87 %, and 0 %, respectively.

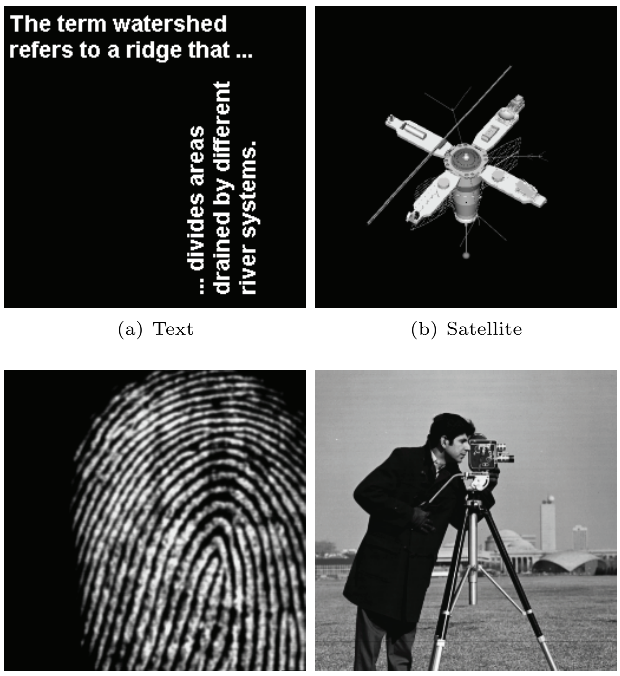

(a) Text (b) Satellite

(c) Fingerprint (d) Cameraman

Fig. 1 Test images

We compare APEA-BCTV with the other three TV-based methods. The first one is also an ADMM based box-constrained algorithm denoted by CTY[8]. The major difference between our algorithm and CTY is that, our algorithm achieves the automatic estimation of the regularization parameter so that it can operate without manual interference, whereas the regularization parameter in CTY is predetermined manually by try-and-error. The second one is a simplified edition of the APEA-BCTV with no box constraints, denoted by APEA-TV. The deduction of APEA-TV is similar to that of APEA-BCTV, and for simplicity, we do not give it here. The third one is a primal-dual model based method with automatic regularization parameter estimation but without box constraints, denoted by Wen and Chan[15]. The code for CTY was coded by us and the code for Wen and Chan was provided by the authors.

We make use of the Matlab commands "fspecial (Gaussian, [9 9], 3)" and "fspecial (average, 9)" to blur the four test images first. Then the solutions are further corrupted by Gaussian noise such that the BSNRs of the observed images are 20 dB, 30 dB, and 40 dB, respectively. The stopping criterion for all methods is $\|\boldsymbol{u}^{k+1}-\boldsymbol{u}^{k}\|_2^2/\|\boldsymbol{u}^{k}\|_2^2 \le 10^{-6}$ or the number of iterations is larger than 1 000, where $\boldsymbol{u}^k$ is the restored image in the kth iteration.

Tables 1 and 2 present the ISNRs and the runtimes of the different algorithms under the Gaussian blur and the average blur, respectively. We use the bold type numbers to represent the best results. From Table 1, we observe that under the Gaussian blur, APEA-BCTV is competitive with CTY in terms of ISNR and both are better than the other two algorithms without box constraints. Under the average blur in Table 2, APEA-BCTV does not perform as well as CTY in terms of ISNR but the results of the two algorithms are close. We should emphasize that when executing CTY, one should try many times to find the approximately optimal regularization parameter to guarantee the accuracy of the solution. This work will cost much more extra time, since the regularization parameter is sensitive to image type, blur kernel, and noise level. For instance, under the average blur, we should set the regularization parameter as large as 2 000 for "cameraman" image with a BSNR of 40 dB, but as little as 5 for "satellite" image with a BSNR of 20 dB for CTY. Besides, adjusting the regularization parameter manually is not allowed in many practical applications. Compared with CTY, APEA-BCTV selects the regularization parameter adaptively. If we treat the ISNRs produced by CTY as the reference, the ISNRs given by APEA-BCTV are reasonable enough.

Tables 1 and 2 also show that box constraints are much more effective and necessary for image whose percentage of extreme-value pixels is high, such as images "text" and "satellite". In particular, for image "text" blurred by the average kernel with a BSNR of 40 dB, the restored ISNRs

Table 1 Comparison in terms of ISNR and runtime for image restorations from Gaussian blurring observations

		ISNR (dB)				Runtime (s)			
BSNR (dB)	Images	APEA-BCTV	CTY	APEA-TV	Wen and Chan	APEA-BCTV	CTY	APEA-TV	Wen and Chan
20	(a)	6.24	**6.26**	4.05	4.09	13.18	11.18	**5.17**	17.12
	(b)	**3.74**	3.67	3.07	2.76	12.54	10.90	**2.98**	16.74
	(c)	4.18	**4.22**	4.06	3.90	11.45	9.82	**4.24**	16.62
	(d)	**2.72**	2.70	2.64	2.58	10.51	8.92	**1.70**	16.08
30	(a)	11.18	**11.21**	7.04	7.38	13.38	11.81	**4.71**	16.95
	(b)	4.62	**4.71**	3.97	3.53	13.32	11.38	**2.67**	16.37
	(c)	**6.52**	6.46	6.41	6.05	11.24	9.92	**3.77**	16.59
	(d)	**4.23**	4.08	4.18	4.05	10.46	8.82	**1.50**	10.64
40	(a)	17.70	**18.83**	10.43	11.39	13.40	11.83	**4.77**	15.02
	(b)	**6.65**	6.62	5.24	5.23	12.96	11.53	**2.46**	16.29
	(c)	9.43	**9.46**	9.41	8.56	11.43	9.68	**3.18**	16.25
	(d)	**6.34**	**6.34**	6.33	6.21	10.36	8.84	**1.30**	8.51

Table 2 Comparison in terms of ISNR and runtime for image restorations from average blurring observations

		ISNR (dB)				Runtime (s)			
BSNR (dB)	Images	APEA-BCTV	CTY	APEA-TV	Wen and Chan	APEA-BCTV	CTY	APEA-TV	Wen and Chan
20	(a)	9.05	**9.24**	6.01	6.24	13.00	11.69	**5.67**	17.05
	(b)	4.46	**4.50**	3.79	3.78	12.77	11.01	**2.73**	16.82
	(c)	4.09	**4.27**	3.85	3.87	11.10	9.82	**3.23**	16.31
	(d)	**3.93**	3.91	3.92	3.85	10.55	8.77	**1.61**	13.48
30	(a)	**17.37**	17.26	10.21	10.71	13.50	10.44	**4.61**	13.95
	(b)	6.06	**6.25**	5.51	5.41	13.08	11.64	**2.43**	15.73
	(c)	7.07	**7.15**	6.63	6.45	11.20	9.94	**3.01**	16.18
	(d)	**5.92**	**5.92**	5.89	5.86	8.10	8.80	**1.40**	8.91
40	(a)	26.79	**27.35**	16.41	16.10	13.53	11.84	**1.30**	9.63
	(b)	**9.30**	9.29	7.72	7.83	13.06	10.96	**2.16**	8.35
	(c)	10.41	**10.85**	10.05	10.03	11.54	9.72	**2.38**	10.33
	(d)	8.62	**8.65**	8.60	8.46	7.26	8.80	**1.27**	6.14

of APEA-BCTV and CTY are at least 10 dB higher than those of APEA-TV and Wen and Chan. For image "satellite" blurred by the Gaussian kernel with a BSNR of 20 dB, the gain in ISNR of algorithm CTY over the other two algorithms is still at least 0.6 dB, which is the least for images "text" and "satellite". In contrast, for test images "fingerprint" and "cameraman", whose percentages of extreme-value pixels are not high, the gain in ISNR of APEA-BCTV or CTY over APEA-TV or Wen and Chan is not obvious in most cases.

Furthermore, in terms of speed, APEA-TV outperforms the other three remarkably. The proposed APEA-BCTV is a little slower than CTY, since the estimation of the regularization parameter costs some extra time. The reason why APEA-BCTV and CTY are much slower than APEA-TV is obvious: the box constraints make the convergence slower. Compared with Wen and Chan, APEA-BCTV is faster in most cases, since Wen and Chan involves inner iterations to achieve the automatic estimation of the regularization parameter, whereas APEA-BCTV involves no inner iteration.

Fig. 2 shows the observed "text" image blurred by the Gaussian kernel with a BSNR of 20 dB, and the restored results of the four algorithms. From Fig. 2, we can visually find that the restorations of APEA-BCTV and CTY are on the same level, both remarkably outperforming the restorations of APEA-TV and Wen and Chan. The similar phenomenon can be found in the other restoration results of images "text" and "satellite". This illustrates the effectiveness of box constraints for image with high percentage of extreme-value pixels. On the contrary, the results shown in Fig. 3 indicate that the gain in ISNR and visual quality of box constraints over no box constraint is not obvious for the test image "cameraman", which possesses a 0 % percentage of extreme-value pixels.

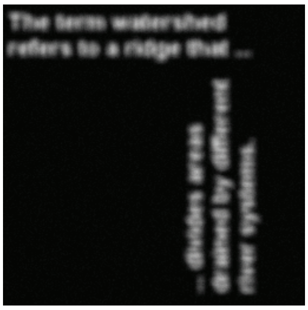

(a) Blurred

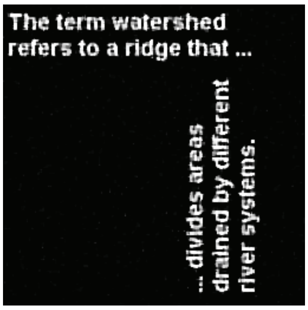

(b) APEA-BCTV

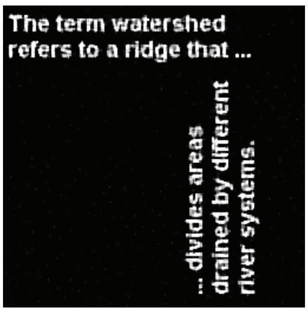

(c) CTY

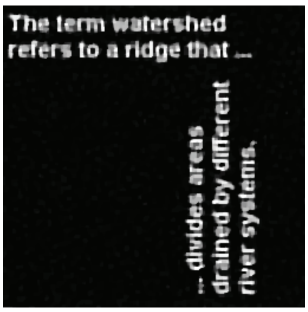

(d) APEA-TV

(e) Wen and Chan

Fig. 2 Observed and restored "text" images ((a) observed "text" image which is degraded by a 9 × 9 Gaussian blur with a BSNR of 20 dB, and the restored images by (b) APEA-BCTV, (c) CTY, (d) APEA-TV and (e) Wen and Chan, with ISNRs of 6.24 dB, 6.26 dB, 4.05 dB, and 4.09 dB, respectively.)

(a) Blurred

(b) APEA-BCTV

(c) CTY

(d) APEA-TV

(e) Wen and Chan

Fig. 3 Observed and restored "cameraman" images ((a) observed "cameraman" image which is degraded by a 9 × 9 average blur with a BSNR of 30 dB, and the restored images by (b) APEA-BCTV, (c) CTY, (d) APEA-TV and (e) Wen and Chan, with ISNRs of 5.92 dB, 5.92 dB, 5.89 dB, and 5.86 dB, respectively.)

4 Conclusion

We have developed an ADMM based algorithm to automatically solve the TV image restoration problem with box constraints. Unlike the existing methods dealing with box constraints, our algorithm achieves the automatic estimation of the regularization parameter without inner iteration. In each iteration, the update of the regularization parameter is in a closed form. Numerical experiments in image restoration indicate that our algorithm produces more accurate solutions, especially for those images with high percentages of extreme-value pixels.

Acknowledgement

The authors would like to acknowledge Dr. SI Xiao-Sheng for his useful suggestion in English writing, and Professor WEN You-Wei for providing the Matlab code of [15].

References

1 Campisi P, Egiazarian K. *Blind Image Deconvolution-Theory and Applications*. Boca Raton: CRC Press, 2007. 1−32

2 Rudin L, Osher S, Fatemi E. Nonlinear total variation based noise removal algorithms. *Physica D*, 1992, **60**(1−4): 259−268

3 Wang Xu-Dong, Feng Xiang-Chu, Huo Lei-Gang. Iteratively reweighted anisotropic-TV based multiplicative noise removal model. *Acta Automatica Sinica*, 2012, **38**(3): 444−451 (in Chinese)

4 Kim D, Sra S, Dhillon I S. Tackling box-constrained optimization via a new projected quasi-Newton approach. *SIAM Journal on Scientific Computing*, 2010, **32**(6): 3548−3563

5 Morini B, Pocelli M, Chan R H. A reduced Newton method for constrained linear least-squares problems. *Journal of Computational and Applied Mathematics*, 2010, **233**(9): 2200−2212

6 Becky A, Teboulle M. Fast gradient-based algorithms for constrained total variation image denoising and deblurring problems. *IEEE Transactions on Image Processing*, 2009, **18**(11): 2419−2434

7 Chan R H, Ma J. A multiplicative iterative algorithm for box-constrained penalized likelihood image restoration. *IEEE Transactions on Image Processing*, 2012, **21**(7): 3168−3181

8 Chan R H, Tao M, Yuan X M. Constrained total variation deblurring models and fast algorithms based on alternating direction method of multipliers. *SIAM Journal on Imaging Sciences*, 2013, **6**(1): 680−697

9 Ma J. Multiplicative algorithms for maximum penalized likelihood inversion with non-negative constraints and generalized error distributions. *Communications in Statistics-Theory and Methods*, 2006, **35**(5): 831−848

10 Ma J. Positively constrained multiplicative iterative algorithm for maximum penalized likelihood tomographic reconstruction. *IEEE Transactions on Nuclear Science*, 2010, **57**(1): 181−192

11 Chan R H, Liang H X, Ma J. Positively constrained total variation penalized image restoration. *Advances in Adaptive Data Analysis*, 2011, **3**(1−2): 187−201

12 Wen Y W, Yip A M. Adaptive parameter selection for total variation image deconvolution. *Numerical Mathematics-Theory Methods and Applications*, 2009, **2**(4): 427−438

13 Ng M, Weiss P, Yuan X. Solving constrained total-variation image restoration and reconstruction problems via alternating direction methods. *SIAM Journal on Scientific Computing*, 2010, **32**(5): 2710−2736

14 Afonso M V, Bioucas-Dias J M, Figueiredo M A T. An augmented Lagrangian approach to the constrained optimization formulation of imaging inverse problems. *IEEE Transactions on Image Processing*, 2011, **20**(3): 681−695

15 Wen Y W, Chan R H. Parameter selection for total-variation-based image restoration using discrepancy principle. *IEEE Transactions on Image Processing*, 2012, **21**(4): 1770−1781

16 Blomgren P, Chan T F. Modular solvers for image restoration problems using the discrepancy principle. *Numerical Linear Algebra with Applications*, 2002, **9**(5): 347−358

17 Liao H Y, Li F, Ng M K. Selection of regularization parameter in total variation image restoration. *Journal of the Optical Society of America A-Optics Image Science and Vision*, 2009, **26**(11): 2311−2320

18 Engl H W, Grever W. Using the *L*-curve for determining optimal regularization parameters. *Numerische Mathematik*, 1994, **69**(1): 561−580

19 An Yao-Zu, Lu Yao, Zhao Hong. An adaptive-regularized image super-resolution. *Acta Automatica Sinica*, 2012, **38**(4): 601−608 (in Chinese)

20 Lin Y Z, Wohlberg B, Guo H B. UPRE method for total variation parameter selection. *Signal Processing*, 2010, **90**(8): 2546−2551

21 Chambolle A. An algorithm for total variation minimization and applications. *Journal of Mathematical Imaging and Vision*, 2004, **20**(1−2): 89−97

22 He B S, Yuan X M. Convergence analysis of primal-dual algorithms for a saddle-point problem: from contraction perspective. *SIAM Journal on Imaging Sciences*, 2012, **5**(1): 119−149

23 Papadakis N, Peyré G, Oudet D. Optimal transport with proximal splitting. *SIAM Journal on Imaging Sciences*, 2014, **7**(1): 212−238

24 Zhang Wen-Juan, Feng Xiang-Chu, Wang Xu-Dong. Mumford-Shah model based on weighted total generalized variation. *Acta Automatica Sinica*, 2012, **38**(12): 1913−1922 (in Chinese)

25 Raguet H, Fadili J, Peyré G. A generalized forward-backward splitting. *SIAM Journal on Imaging Sciences*, 2013, **6**(3): 1199−1226

26 Xue Qian, Yang Cheng-Yi, Wang Hua-Xiang. Alternating direction method for salt-and-pepper denoising. *Acta Automatica Sinica*, 2013, **39**(12): 2071−2076 (in Chinese)

27 Wu C L, Tai X C. Augmented Lagrangian method, dual methods, and split Bregman iteration for ROF, vectorial TV, and high order models. *SIAM Journal on Imaging Sciences*, 2010, **3**(3): 300−339

28 Wang Y L, Yang J F, Yin W T, Zhang Y. A new alternating minimization algorithm for total variation image reconstruction. *SIAM Journal on Imaging Sciences*, 2008, **1**(3): 248−272

29 Combettes P L, Pesquet J C. *Fixed-point Algorithms for Inverse Problems in Science and Engineering — Chapter 10: Proximal Splitting Methods in Signal Processing*. New York: Springer, 2011. 185−212

HE Chuan Ph. D. candidate at Hi-Tech Institute of Xi′an. His research interest covers signal/image processing and remote sensing. Corresponding author of this paper. E-mail: hechuan8512@163.com

HU Chang-Hua Cheung Kong professor at Hi-Tech Institute of Xi′an. He was a visiting scholar at the University of Duisburg-Essen, Germany from September 2008 to December 2008. His research interest covers fault diagnosis and prediction, life prognosis, and fault tolerant control.
E-mail: hch6603@263.net

ZHANG Wei Associate professor at Hi-Tech Institute of Xi′an. Her research interest covers pattern recognition and communication technology.
E-mail: zhang1966wei@163.com

SHI Biao Postdoctor at Hi-Tech Institute of Xi′an. His research interest covers signal/image processing and remote sensing with terahertz wave.
E-mail: biaosh2008@163.com